E-23
Kongres 2026
Congress 2026

doi: 10.67563/ASESCONF2026073S

Radmila Sinđić Grebović[1], Mina Grebović[2]

NUMERICAL ANALYSIS OF A NON-SLENDER HIGH-STRENGTH CONCRETE BEAM USING ABAQUS

Summary: The shear design of non-slender reinforced high-strength concrete (HSC) beams remains questionable, as indicated by experimental findings. This paper aims to perform a numerical simulation of a non-slender HSC beam and compare the results with experimental data. A finite element model of the tested HSC beam was developed in Abaqus, incorporating the properties as specified in the experimental study. The numerical results are compared with experimentally obtained ultimate load and observed failure mode, as well as with results derived from the simple and refined Strut-and-Tie Model (STM). The comparison shows reasonable agreement between numerical and experimental responses, while certain differences are observed relative to STM predictions. The study demonstrates that finite element modeling can serve as a useful complementary tool for evaluating the shear behavior of non-slender beams and for assessing the reliability of STM in practical design.

Keywords: high-strength concrete, strut-and-tie model, non-slender beam, shear, Abaqus, finite element analysis

NUMERIČKA ANALIZA NEVITKE GREDE OD BETONA VISOKE ČVRSTOĆE PRIMJENOM ABAQUS-A

Rezime: Proračun smičuće nosivosti nevitkih armiranobetonskih greda od betona visoke čvrstoće (HSC) i dalje je upitan, na šta ukazuju eksperimentalni podaci. Cilj ovog rada je sprovođenje numeričke simulacije nevitke HSC grede i poređenje dobijenih rezultata sa eksperimentalnim podacima. Model konačnih elemenata ispitivane HSC grede razvijen je u softverskom paketu Abaqus, uz uvrštavanje svojstava specifikovanih u eksperimentalnom ispitivanju. Numerički rezultati su upoređeni sa eksperimentalno dobijenom graničnom nosivošću i osmotrenim oblikom loma, kao i sa rezultatima izvedenim primjenom jednostavnog i rafinisanog modela pritisnutih dijagonala i zategnutih veza (STM). Poređenje pokazuje razumno poklapanje između numeričkih i eksperimentalnih odgovora, dok su određene razlike uočene u odnosu na predikcije dobijene primjenom STM-a. Studija pokazuje da modeliranje metodom konačnih elemenata može poslužiti kao koristan komplementarni alat za procjenu ponašanja nevitkih greda pri smicanju i za ocjenu pouzdanosti STM-a u praktičnom projektovanju.

Ključne riječi: beton visoke čvrstoće, strut-and-tie model, nevitka greda, smicanje, Abaqus, analiza konačnih elemenata

[1] Faculty of Civil Engineering, University of Montenegro
[2] Faculty of Civil Engineering, University of Montenegro, minag@ucg.ac.me

1. INTRODUCTION

Shear resistance design in reinforced concrete beams has posed a persistent challenge in construction for over a century, largely due to the lack of a universally accepted analytical solution. Early shear models by Ritter and Mörsch were regarded as conservative and were missing essential impact factors [1]. However, the adoption of less stringent ACI 1920 rules resulted in unsafe designs and contributed to the unpredictable, brittle failure of warehouse beams in 1955 [2]. It is shown that shear failure in beams without shear reinforcement can occur without warning, with the clear opening of a major diagonal crack. Consequently, research shifted toward investigating shear transfer mechanisms and reliability, leading to the introduction of B and D regions in the late 1980s [1], [2]. The design of beams in flexure may be based on the sectional moment, assuming the Bernoulli hypothesis, in which the plane section after bending remains plane, and the strain is linearly distributed across the section, in the area called the B-region. It is based on truss models.

Beams are generally categorized as either slender or deep (non-slender). Slenderness is determined by the shear span-to-depth ratio (a/d), where a is the shear span and d is the beam's effective depth. According to standard structural terminology, elements with a shear span-to-depth ratio below 2.4 are classified as non-slender members [3], [4], [5]. This behavior is fundamentally distinct from that of slender beams.

These concrete beams are structural elements whose behavior is governed by discontinuity zones (D-regions) that arise from sudden changes in concentrated loads (static discontinuity) or in geometry (geometric discontinuity). In the D-region, load-transfer mechanisms cannot be accurately described by classical beam theory or standard sectional shear approaches because significant nonlinear strain distributions occur within the cross-section.

Over the past fifty years, various approaches to D-region modeling have been proposed. Many experimental studies have been conducted to validate empirical equations, but no adequate theory exists for potentially more dangerous members without shear reinforcement [5]. For members with significant amounts of shear reinforcement, a variable-angle truss model based on the lower-bound theory of plasticity is incorporated into worldwide code provisions [2], [3], [4]. The current version of Eurocode 2 (EN1992-1-1:2004) recommends strut-and-tie modeling for D-regions and limits compressive stress as a function of concrete strength only [6].

Many experimental studies on these topics focus on this theme. Investigations of the effectiveness factor for predicting shear strength, based on tests of reinforced non-slender beams, indicate that predictions for shear-reinforced beams have been conservative. In contrast, predictions for beams without shear reinforcement, using the effectiveness factor in Eurocode 2 and ACI 318, yield unreliable and unsafe results [2], [5], [7]. In previous research, the shear capacity of reinforced concrete (RC) non-slender beams has most often been assessed using STM and numerical models (FEM), as shown in Figure 1.

Accordingly, a new generation of Eurocode 2 includes the use of stress fields and their combination with classical strut-and-tie models [8], [9], [10].

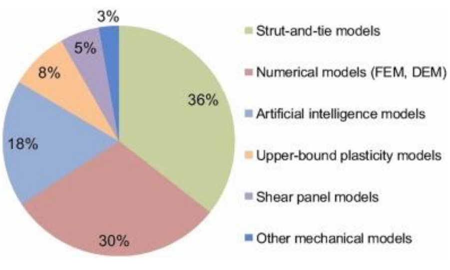

Figure 1: Models of shear capacity used for concrete non-slender beams [7]

The reliability of the STM model's application to Normal-Strength Concrete (NSC), which is defined as concrete with compressive strength up to 50 MPa, has been comprehensively assessed through experimental research. Against that, current provisions for High-Strength Concrete (HSC), defined as classes exceeding C50/60 and standardized up to C100/115 in current codes, exhibit significant limitations and lack comprehensive experimental validation [10]. Further, experimental research demonstrates that HSC elements subjected to shear exhibit brittle failure modes and non-conservative behavior, with a more pronounced size effect [11].

Notable differences in stress-strain characteristics between HSC and normal-strength concrete require modifications to design parameters [8]. Experimental data indicate that existing shear capacity provisions for reinforced concrete beams are not sufficiently reliable, particularly for HSC, where increased compressive strength does not substantially improve shear resistance. Due to the considerable variability in published results, it is essential to verify code-prescribed procedures against experimental data to develop reliable design solutions [7, 11].

2. MATERIAL AND METHODS

This research program focuses on modeling non-slender, HSC beams with concentrated loads near the support to evaluate shear strength in D-regions using numerical methods in ABAQUS, and to compare these results with experimental results and with the STM design proposed in Eurocode 2, EN 1992-1-1:2004, and the new EN 1992-1-1:2023. The program is implemented using part of the experimental results from extensive research on shear in high-strength concrete beams, conducted in the Laboratory of the Faculty of Civil Engineering at the University of Montenegro in Podgorica. This paper presents a numerical model of a beam at the slender-non-slender boundary that was previously experimentally tested. Modeling another 20 HSC beams with shear-span-to-depth ratios ranging from 1.25 to 2.0, using the experimental data repository [12], will be the subject of future research.

2.1. EXPERIMENTAL RESEARCH

The experimental research presented in this paper has been conducted on an HSC beam (LS) with concrete assessed as strength class C 70/85, based on the experimental data. The average 28-day concrete strength of the experimental model is 89 MPa for a 15-cm cube and 81 MPa for a 10/10/40-cm prism [13]. It is tested as a simple beam with a span of 180 cm and a rectangular cross-section of 15/30 cm, under a transverse load consisting of a pair of concentrated forces on the shear span, applied by a support at $a = 66$ cm. Longitudinal reinforcement ratio of 2% in tension ($f_{yk} = 456$ MPa) and 1% in compression. Transverse reinforcement is installed as vertical stirrups, Ø6/20 cm.

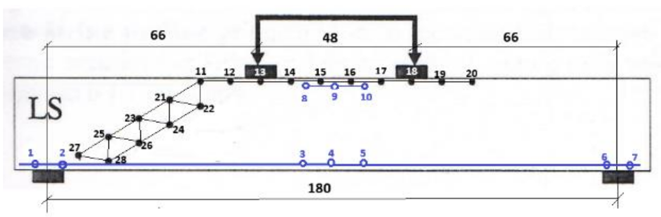

Figure 2: Tested HSC beam with disposition of strain measurement base

The tested beam is loaded with two concentrated forces near the support with a shear-span-to-depth ratio of 2.5. It is designed with minimal transverse reinforcement, consisting of vertical stirrups, to ensure shear failure. The strain gauges and measurement points numbered 1-10 are placed on the longitudinal reinforcement. On the concrete surface, points for mechanical measurement devices are placed spaced 100 mm apart in the D region of the shear zone along the strut (labeled 21-28), arranged along the sides of equilateral triangles. On both faces of the concrete surfaces under the load points along the compression zone due to pure bending, measuring points marked 11-20 were installed. So, measurements were used to record precise strain developments in both concrete and steel, the propagation of diagonal cracks, or the sudden, brittle crushing of concrete struts.

2.2. STRUT-AND-TIE MODEL

The STM idealizes the complex stress field within concrete as an equilibrium system comprising compressive struts, tensile ties, and nodal zones. Based on the lower-bound theorem of plasticity, it is classified as a lower-bound plastic method. Theoretically, this indicates that the estimated ultimate capacity is consistently at or below the actual collapse load [2].

Research shows that the predicted shear strength of non-slender beams is significantly affected by the geometry of the nodal zone [11]. Consequently, the variable and uncertain geometry of the STM introduces uncertainty into structural reliability. Ideally, struts align with compressive stress trajectories, which redistribute after diagonal cracking. Therefore, a refined model should be developed based on the actual crack pattern of the experimentally tested beam. Furthermore, STM can be derived by starting with simple, calculated approaches that cover most design situations and ending with strain-based approaches to obtain more accurate estimates [9].

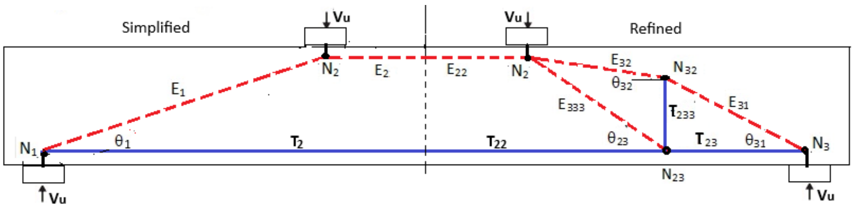

Figure 3: Simplified (left) and refined (right) strut-and-tie models of experimentally tested beam

The simplified STM of the tested beams shown in Figure 3 (left half) consists of two struts connected at node N_2 (type CCC) and one tie connected to the strut at node N_1 (type CCT), which connects two elements in compression and one in tension. STMs, in accordance with both generations of Eurocode 2, were applied to experimentally tested specimens to compare the experimental results with the design.

Table 1: Labeling of R-STM elements; Equations for calculation from equilibrium conditions.

ST Model	Type	ID	Force	Equation
Simplified	Strut	E_1	F_1	$F_1 = V/sin\theta_1$
		E_2	F_2	$F_2 = F_1 \cdot cos\theta_1 = V/tan\theta_1$
	Tie		T_2	$T_2 = -F_2$
Refined	Strut	E_{31}	F_{31}	$F_{31} = V/sin\theta_{31}$
		E_{32}	F_{32}	$F_{32} = F_{31} \cdot cos\theta_{31}/cos\theta_{32}$
		E_{333}	F_{333}	$F_{333} = V/sin\theta_{23} - F_{32} \cdot sin\theta_{32}/sin\theta_{23}$
		E_{22}	F_{22}	$F_{22} = F_{32} \cdot cos\theta_{32} + F_{333} \cdot cos\theta_{23}$
	Tie		T_{22}	$T_{22} = -F_{22}$
			T_{23}	$T_{23} = F_{31} \cdot cos\theta_{31}$
			T_{233}	$T_{233} = F_{333} \cdot sin\theta_{23}$

Eurocode 2 (EN 1992-1-1:2004) recommends limiting the design compressive stress in struts with transverse cracking.

$$\sigma_{Rdmax} = 0{,}6\nu f_{cd} \tag{1}$$

$$\nu = 1 - f_{ck}/250 \tag{2}$$

where:
σ_{Rdmax} is the design compression stress in the strut,
ν is the reduction factor,
f_{cd} is the design concrete compressive strength.

In new Eurocode 2 (EN 1992-1-1:2023), strut-and-tie models are proposed for the design and verification of discontinuity regions. Concrete struts and compression fields are assumed to have uniformly distributed stresses across the cross-section and are calculated using Equation 3 [10].

$$\sigma_{cd} = \frac{|F_{cd}|}{b_c \cdot t} \tag{3}$$

where:
F_{cd} is the compressive force of the strut,
b_c is the thickness of the strut,
t is the width of the strut.

The compressive stress σ_{cd} in the strut shall fulfill the condition in Equation 4:

$$\sigma_{cd} \leq \nu \cdot f_{cd} \tag{4}$$

where:
ν is the reduction factor depending on the angle θ_{cs} between the strut and any of the ties that cross with the strut. It may take any of the constant values prescribed in the code for θ_{cs}. Alternatively, it may be calculated using Equation 5:

$$\nu = 1/(1{,}11 + 0{,}22 \cdot cot^2\theta_{cs}) \tag{5}$$

In cracked zones, the principal tensile strain ε_1 can be determined using Equation 6.

$$\nu = 1/(1{,}0 + 110\varepsilon_1) \tag{6}$$

where:
f_{cd} is the design value of the compression strength of concrete, calculated by Equation 7.

$$f_{cd} = \frac{f_{ck}}{\gamma_c}\eta_{f_c} \tag{7}$$

where:
f_{ck} and γ_c are, respectively, the characteristic compressive cylinder strength and the partial safety factor, while η_{f_c} is a strength reduction factor, which takes into account the post-peak strain-softening behavior of concrete when subjected to uniaxial compression [9].

$$\eta_{f_c} = \left(\frac{40}{f_{ck}}\right)^{\frac{1}{3}} \leq 1 \tag{8}$$

The resistance of a tie composed of non-prestressed reinforcement is

$$F_{td} \leq F_{Rd} = A_s \cdot f_{yd} \tag{9}$$

where A_s and f_{yd} denote the area and yield strength of the reinforcing steel, respectively.

2.3. NUMERICAL MODEL

A two-dimensional nonlinear finite element model (Figure 4) of the reinforced concrete beam was developed in Abaqus/Standard to simulate its structural response under the experimental loading conditions. The model geometry, reinforcement layout, and loading configuration were defined to match the experimentally tested beam, thereby enabling a direct comparison between the numerical and experimental results.

Longitudinal and transverse reinforcement were represented by two-node truss elements (T2D2) with full integration and capable of carrying only axial forces. The concrete was discretized using four-node plane-stress elements (CPS4), with reduced integration disabled [14]. The size of the finite elements in the concrete part of the cross-section was 10×10 mm. The length of the finite elements used for the steel components was 50 mm.

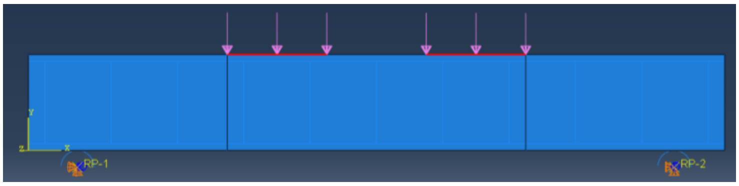

Figure 4: Model of the reinforced high-strength concrete beam

The nonlinear behavior of concrete was simulated using the Concrete Damaged Plasticity (CDP) model. This model enables representation of stiffness degradation due to tensile cracking and compressive crushing using scalar damage variables [15].

Table 2: CDP model parameters

Ψ	ε	f_{bo}/f_{co}	K	μ
31°	0.1	1.16	0.667	1E-06

The damage parameters of the CDP model, including the dilation angle Ψ, eccentricity ε, the ratio of biaxial to uniaxial compressive strength f_{bo}/f_{co}, the shape parameter of the plastic potential K, as well as the viscosity coefficient, were adopted based on recommendations from the literature, as shown in Table 2 [16]. The elastic modulus was taken as E = 44.4 GPa, with a Poisson’s ratio of 0.2. The compressive stress–strain relationship implemented in the CDP model was derived from the experimentally determined mechanical properties of the concrete, shown in Figure 5. Both the longitudinal reinforcement and stirrups were modeled as elastic–plastic steel with isotropic hardening. The elastic modulus was taken as 200 GPa, the Poisson's ratio as 0.30, and the yield strength was determined from the experimentally determined mechanical properties of the reinforcement (Figure 5).

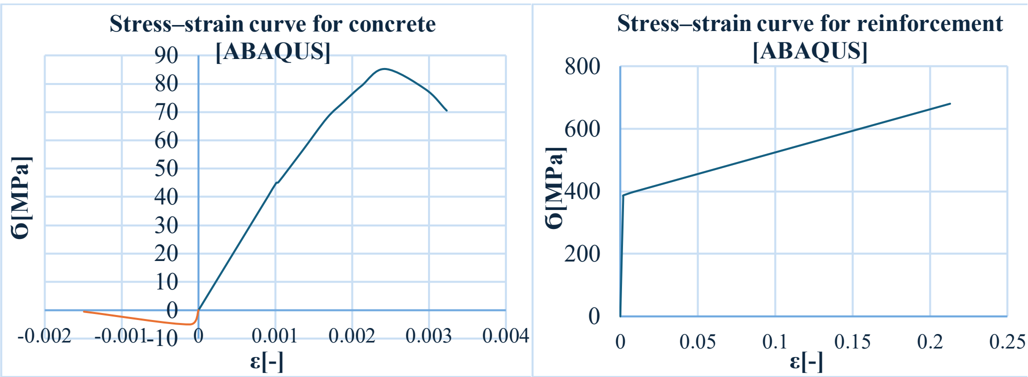

Figure 5: Stress-strain curves for concrete in Abaqus (left) and stress-strain curve for reinforcement in Abaqus (right)

To simulate the progressive deterioration of concrete, tensile and compressive damage parameters (d_t and d_c) were incorporated into the Concrete Damaged Plasticity (CDP) model. These scalar variables range from 0 to 1, where 0 denotes undamaged concrete, and 1 indicates complete material degradation. Within the CDP formulation, cracking is represented using the smeared-crack approach, in which damage is distributed across the finite elements rather than modeled as discrete cracks. Therefore, the tensile damage variable (DAMAGET) was used to visualize crack propagation and assess the agreement between the numerically predicted failure mechanism and the experimentally observed crack pattern. [17]

The interaction between concrete and reinforcement was established using the Embedded Region technique available in Abaqus, which assumes perfect bond between the reinforcement and the surrounding concrete and neglects bond-slip effects. Although this represents a modeling simplification, it is commonly adopted in nonlinear analyses of reinforced concrete members and provides satisfactory accuracy for predicting the global structural response [18].

The supports were modeled as two-dimensional analytical rigid bodies, while the interactions between the beam and the supports and loading plates were modeled using surface-to-surface contact.

The load was applied as a uniformly distributed pressure (Figure 4) acting directly on two predefined loading regions located symmetrically about the beam midspan. Applying the load over finite surface areas, rather than at discrete nodes, prevents unrealistic local stress concentrations and promotes a stable numerical response.

A nonlinear static analysis was carried out using the implicit solution procedure implemented in Abaqus/Standard, accounting for both material and geometric nonlinearities. Automatic load incrementation was adopted to ensure stable convergence as concrete damage progressed. Throughout the analysis, displacements, reaction forces, stresses, strains, and damage variables were monitored to evaluate the structural response and to enable comparison with the experimental observations and the predictions obtained using the strut-and-tie model.

3. RESULTS AND DISCUSSION

Analysis of the experimental results revealed the typical shear failure mechanism of the tested beam. The crack pattern illustrated a strong diagonal-tension crack, indicating a diagonal-tension failure. The ultimate limit transverse shear force registered during testing reached 135 kN.

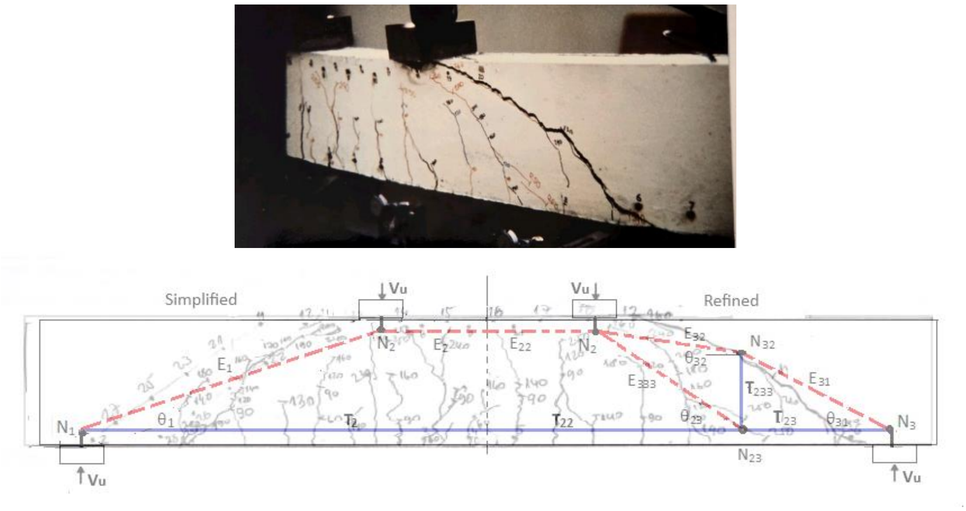

Figure 6: Crack pattern and STM of experimentally tested beam

Table 3 presents the forces in the STM elements, calculated from the model equilibrium, for the experimentally determined ultimate force $V_{u,exp}$. The columns EC2-2004 and EC2-2023 display the forces in the elements of the model assuming that the design capacity of the strut has been reached, while the f_{yd} column shows the forces calculated based on the yielding of the steel tie. The effective strut width and inclination angles are defined based on the geometry of the experimental model. Strains in the longitudinal reinforcement (ε_s) were measured with strain gauges and used in calculations. Values in columns EC2-2004 and EC2-2023 are calculated for the strut's design strength as prescribed by these codes, with an acceptance partial safety factor of $\gamma_c = 1.0$. The overestimated load capacity of the struts for $V_{u,exp}$ is a consequence of the actual failure mode and the pronounced opening of the inclined crack, which does not correspond to the assumed STM or the crack pattern. The analysis results indicate significant differences in the methodologies for defining STM between the current and new Eurocode 2. EC2-2004 prescribes a limiting strut capacity that is solely a function of concrete strength, whereas under EC2-2023, the design capacity also incorporates the inclination angle between the strut element and the tie. It is also evident in the evaluation of the design concrete strength, where EC2-2023 introduces a new correction factor that is particularly significant for concrete classes higher than C40/50.

It is shown that EC2-2004 does not provide a reliable estimate of the strut design capacity, as it relies on the same strut capacity value across different models and shear capacities. Conversely, by adapting the model parameters, the new EC2-2023 enables more reliable predictions of the strut's ultimate capacity by applying an appropriate STM, including stress-field analysis.

Table 3: Comparison of actual strut forces for ultimate measured load $V_{u,exp}$, design forces by EC2–2004 and EC2–2023, and yielding force in tie

ST Model	t [mm]	b_c [mm]	Forces	$V_{u,exp}$ [kN]	EC2 – 2004 [kN]	EC2 – 2023 [kN]	f_{yd} [kN]
Simplified	150	100	F_1	437.1	385.6	272.6	384.4
	150	100	F_2	415.7	366.7	259.3	365.6
			T_2	415.7	366.7	259.3	365.6
			V	135.0	119.1	84.2	118.7
Refined	150	100	F_{31}	297.5	385.6	444.9	265.2
	150	100	F_{32}	267.7	347.0	400.4	238.6
	150	100	F_{333}	174.9	226.7	261.6	155.9
	150	100	F_{22}	410.1	531.5	613.4	365.6
			T_{22}	410.1	531.5	613.4	365.6
			T_{23}	265.1	343.6	396.5	236.3
			T_{233}	97.8	126.7	146.2	87.1
			V	135.0	175.0	201.9	120.3

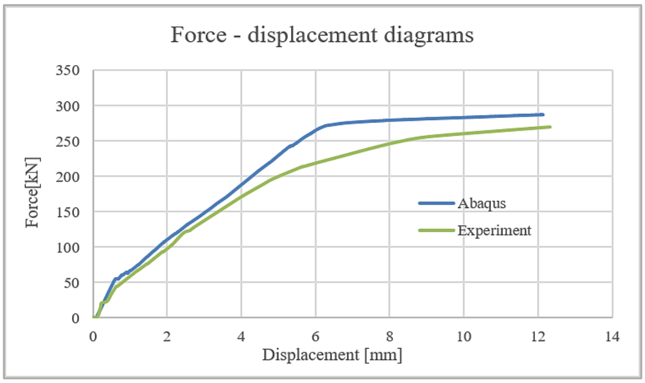

Figure 7: Experimental and numerical force–displacement curves

As shown in Figure 7, the numerical model reproduces the general trend of the experimental force-displacement response. A slightly higher stiffness and ultimate load are observed in the numerical results.

A rapid increase in diagonal tensile damage is observed over the same load range in which the experimental beam exhibited rapid propagation of diagonal shear cracks (Figure 8). With increasing load, the failure mechanism shifts from flexural cracking to the rapid propagation of dominant diagonal shear cracks, which ultimately govern the beam response. This agreement indicates that the numerical model successfully captures not only the ultimate failure mode but also the evolution of cracking.

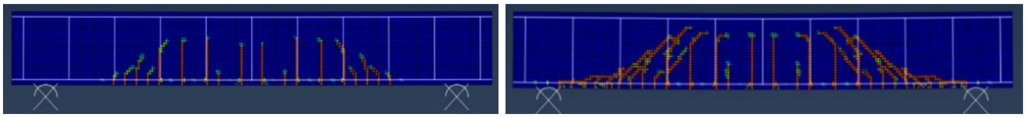

(a) (b)

Figure 8: Evolution of the tensile damage pattern (DAMAGET) in the numerical model at (a) 114 kN and (b) 250 kN, illustrating the initiation and propagation of diagonal shear cracking

The predicted ultimate load deviated by only 5.6% from the experimental result, indicating that the developed FE model provides a satisfactory prediction of the beam's load-carrying capacity (Table 4).

Table 4: Comparison of key experimental and numerical results

Parameter [kN]	Experiment	FEM	Difference [%]
Ultimate load, P_u	270	286	5.6
Initiation of diagonal shear cracking	160	168	4.7
Load at longitudinal reinforcement yielding	240	268	10

In the experimental test, the onset of diagonal shear cracking could not be associated with a single load level, as the diagonal cracks evolved progressively from the existing flexural cracks. Despite this, the numerical model predicted the initiation of diagonal shear cracking within the same loading interval observed experimentally.

Both the experimental observations and the numerical analysis indicate that the longitudinal reinforcement yielded only during the final stages of loading (Table 4). This suggests that the tensile reinforcement capacity was not fully utilized and confirms that the beam failure was governed by shear rather than flexure.

4. CONCLUSION

The following conclusions can be drawn from this study:

- The STM is always an option for discontinuity regions (D-regions), but defining an adequate model is a particularly demanding process that requires complex engineering knowledge and experience. Modern codes provide models that incorporate stress field analysis, establishing rules that explicitly address the assessment of existing structures as well as design purposes. The significant improvements introduced in EN 1992-1-1:2023 compared to EN 1992-1-1:2004 include an assessment of strut resistance.

- A satisfactory agreement between the experimental and numerical force-displacement curves was achieved, with comparable initial stiffness and overall response, confirming the ability of the developed finite element model to represent the global behavior of the tested beam accurately.

- The quantitative comparison between the experimental and numerical results demonstrated the accuracy of the developed finite element model. The ultimate load was predicted with a deviation of only 5.6%, confirming the reliability of the adopted modeling approach.

- The numerical model successfully reproduced the experimentally observed failure mechanism. Both the evolution of diagonal shear cracking and the late yielding of the longitudinal reinforcement were captured with good agreement, confirming the model's ability to simulate the shear response of the tested beam realistically.

REFERENCES

[1] Schlaich J, Schäfer K, Jennewein M. Towards a consistent design of structural concrete, Prestressed Concrete Institute Journal, 32 (3), 1987, 74–150. https://doi.org/10.15554/pcij.05011987.74.150

[2] Collins M.P, Bentz E.C, Sherwood E.G, et al. An adequate theory for the shear strength of reinforced concrete structures. Morley Symposium on Concrete Plasticity and its Application. University of Cambridge, 2007. https://www.researchgate.net/publication/237411162.

[3] Reineck, K. H., & Todisco, L. (2014). Database of Shear Tests for Non-Slender Reinforced Concrete Beams without Stirrups. *ACI Structural Journal*, *111*(6)

[4]Todisco, L., Reineck, K. H., & Bayrak, O. (2015). Database with shear tests on non-slender reinforced concrete beams with vertical stirrups. *ACI Structural Journal*, *112*(6), 761.

[5] Liu J, Mihaylov B.I. A comparative study of models for shear strength of reinforced concrete deep beams, Engineering Structures, 112, 2016, 81–89, https://doi.org/10.1016/j.engstruct.2016.01.012

[6] EN 1992-1-1 Eurocode 2: Design of concrete structures - Part 1-1: General rules and rules for buildings. CEN-CENELEC Management Centre: Brussels, 2004.

[7] Abbood I. S. Strut-and-tie model and its applications in reinforced concrete deep beams: A comprehensive review, Case Studies in Construction Materials, 2023, *19*, e02643. https://doi.org/10.1016/j.cscm.2023.e02643

[8] Muttoni A, Fernández R.M, Niketic F. Design versus Assessment of Concrete Structures Using Stress Fields and Strut-and-Tie Models, Structural Journal, 2015, 112 (5), 605-616. https://doi.org/10.14359/51687710

[9] Fernández Ruiz M, Hoang L.C, Muttoni A. Stress Fields and Strut-and-Tie Models as a Basic Tool for Design and Verification in Second Generation of Eurocode 2, Hormigón y Acero 74(299-300), 2023, 79-90, https://doi.org/10.33586/hya.2022.3086

[10]EN 1992-1-1:2023, Eurocode 2 - Design of concrete structures - Part 1-1: General rules and rules for buildings, bridges and civil engineering structures, CEN, 2023.

[11] Mitchell D, Collins M. P. Revision of Strut-and-Tie Provisions in the AASHTO LRFD Bridge Design Specifications, Project No. NCHRP 20-07/Task 306, 2013, 80.

[12] Sinđić Grebović R. Uticaj visoke čvrstoće betona na smičuću nosivost armiranobetonskih greda, PhD Thesis, University of Montenegro, 2009, http://eteze.ucg.ac.me/

[13] Sinđić Grebović R. Parametarska analiza betona visoke čvrostoće, Master's Thesis, University of Belgrade, 1997.

[14] Dassault Systèmes. Abaqus: Getting started with Abaqus—Interactive edition. Dassault Systèmes Simulia Corp., 2017.

[15] Dassault Systèmes. Abaqus analysis user's manual (v6.6): Section 18.5.3 Concrete damaged plasticity, Dassault Systèmes Simulia Corp., 2017.

[16] Hafezolghorani M., Hejazi F., Vaghei R., Jaafar M.S.B., Karimzade K. Simplified damage plasticity model for concrete. Computers and Concrete, 20(2), 2017, 257–272. https://doi.org/10.2749/101686616x1081

[17] Bahij S., Adekunle S.K., Al-Osta M., Ahmad S., Al-Dulaijan S.U., Rahman M.K. Numerical investigation of the shear behavior of reinforced ultra-high-performance concrete beams. Structural Concrete, 19(1), 2018, 305–317. https://doi.org/10.1002/suco.201700062

[18] Dassault Systèmes. Abaqus Analysis User's Guide: Embedded Elements. Abaqus Documentation, Section 35.4.1. Embedded elements. Dassault Systèmes Simulia Corp., 2023.